International Journal of Chemical, Materials and Biomolecular Sciences
ISSN: 2415-6620
Vol:11, No:6, 2017

Effect of Manganese Doping on Ferroelectric Properties of $(K_{0.485}Na_{0.5}Li_{0.015})(Nb_{0.98}V_{0.02})O_3$ Lead-Free Piezoceramic

Chongtham Jiten, Radhapiyari Laishram, K. Chandramani Singh

***Abstract*—**Alkaline niobate $(Na_{0.5}K_{0.5})NbO_3$ ceramic system has attracted major attention in view of its potential for replacing the highly toxic but superior lead zirconate titanate (PZT) system for piezoelectric applications. Recently, a more detailed study of this system reveals that the ferroelectric and piezoelectric properties are optimized in the Li- and V-modified system having the composition $(K_{0.485}Na_{0.5}Li_{0.015})(Nb_{0.98}V_{0.02})O_3$. In the present work, we further study the pyroelectric behaviour of this composition along with another doped with Mn^{4+}. So, $(K_{0.485}Na_{0.5}Li_{0.015})(Nb_{0.98}V_{0.02})O_3 + x$ MnO_2 (x = 0, and 0.01 wt. %) ceramic compositions were synthesized by conventional ceramic processing route. X-ray diffraction study reveals that both the undoped and Mn^{4+}-doped ceramic samples prepared crystallize into a perovskite structure having orthorhombic symmetry. Dielectric study indicates that Mn^{4+} doping has little effect on both the Curie temperature (T_c) and tetragonal-orthorhombic phase transition temperature (T_{ot}). The bulk density, room-temperature dielectric constant (ε_{RT}), and room-c The room-temperature coercive field (E_c) is observed to be lower in Mn^{4+} doped sample. The detailed analysis of the *P-E* hysteresis loops over the range of temperature from about room temperature to T_{ot} points out that enhanced ferroelectric properties exist in this temperature range with better thermal stability for the Mn^{4+} doped ceramic. The study reveals that small traces of Mn^{4+} can modify $(K_{0.485}Na_{0.5}Li_{0.015})(Nb_{0.98}V_{0.02})O_3$ system so as to improve its ferroelectric properties with good thermal stability over a wide range of temperature.

***Keywords*—**Ceramics, dielectric properties, ferroelectric properties, lead-free, sintering, thermal stability.

I. Introduction

FOR several decades, PZT has been widely used as piezoelectric materials, in actuators, transducers and sensors, because of its superior piezoelectric properties [1]. In recent time, however, there have been serious restrictions imposed by many countries in the use of PZT in electrical appliances because of the environmental concerns caused by lead (Pb) toxicity. This has necessitated the urgent requirement for a lead-free piezoelectric material whose properties match with those of PZT family. As a consequence, there has been a widespread research in recent years to find alternative lead-free piezoelectric ceramics with properties comparable to their lead-based counterparts. In order to find a replacement for lead-based piezoelectrics, attempts have been being made towards developing several lead-free piezoelectric materials such as potassium sodium niobate (KNN)-based ceramics [2]-[4], bismuth sodium titanate-based ceramics [5]-[7], bismuth potassium titanate-based ceramics [8], [9], ferroelectric ceramics with a tungsten bronze structure [10], and bismuth layer-structured ferroelectrics [11]-[13]. Among the alkaline niobate-based perovskite-type ceramics, alkaline niobate system with the composition $(K_{0.5}Na_{0.5})NbO_3$ (KNN) has been reported in literature as one of the most promising candidates because of its good piezoelectric properties, high Curie temperature (T_c) of over 400 °C and low anisotropy [14], [15]. In spite of these merits, KNN ceramics suffer from certain shortcomings such as the need for special handling of the starting powders, sensitivity of properties to non-stoichiometry, and complex densification process [16]. To get well-sintered pure KNN ceramics is extremely difficult under ordinary conditions due to evaporation of K_2O and Na_2O at high temperatures [14], [17]. Therefore, non-conventional methods like spark plasma sintering, templated grain growth and hot isostatic pressing have been used to achieve the desired high densities in KNN ceramics [18]-[20]. These techniques are meant for academic interest only and not suitable for large-scale production in required in industry. There are also other methods to improve the sinterability of KNN ceramics, for instance, the formation of a new solid solution of KNN with other perovskite compounds, such as $LiTaO_3$ [21], use of novel sintering aids like $K_4CuNb_8O_{23}$ [22], and preparation from nanoscale powders [23]. Optimum substitutions of A-site ions $(K_{0.5}Na_{0.5})^+$ and B-site ion Nb^{5+} by other suitable ions in the ABO_3-type perovskite structure of KNN have been reported to enhance its piezoelectric properties [24]-[26]. Gaur et al. reported that the substituted KNN ceramic having the composition $(K_{0.485}Na_{0.5}Li_{0.015})(Nb_{0.88}Ta_{0.1}V_{0.02})O_3$ possesses the optimum values of room-temperature dielectric constant (ε_{RT}), and remnant polarization (P_r), and piezoelectric charge coefficient (d_{33}) [27]. In the present work, we further study $(K_{0.485}Na_{0.5}Li_{0.015})(Nb_{0.98}V_{0.02})O_3$ and also investigate the effect of adding MnO_2 into it. We use MnO_2 as it is widely reported to have a beneficial effect on the electrical properties of piezoelectric ceramics such as $BaTiO_3$ and PZT [28], [29].

Chongtham Jiten is with the Department of Physics, Kirori Mal College, University of Delhi, Delhi -110007, India

Radhapiyari Laishram is with Solid State Physics Laboratory, Lucknow Road, Timarpur, Delhi – 110054, India

K. Chandramani Singh is with the Department of Physics, Sri Venkateswara College, University of Delhi, New Delhi-110021, India (e-mail: kongbam@gmail.com).

II. Materials and Methods

$(K_{0.485}Na_{0.5}Li_{0.015})(Nb_{0.98}V_{0.02})O_3 + x$ MnO_2 (x = 0, and 0.03

wt. %) powders were synthesized by conventional solid state reaction method from the raw materials: K_2CO_3 (99.0%), Na_2CO_3 (99.9%), Li_2CO_3 (99.0%), Nb_2O_5 (99.5%), V_2O_5 (98.5%), and MnO_2(99.5%). They were weighed as per the stoichiometric formula and homogeneously mixed for 15h in a plastic bottle using an ordinary ball mill with isopropanol and zirconia balls as milling media. The mixture was calcined at 850 °C for 4h. The calcined powder was then high-energy milled in isopropanol medium using a Retsch PM 100 planetary ball mill at the speed of 250 rpm for 5h using agate vial and balls. A mass ratio of 1:5 for powder and balls was always maintained during milling. The rotational direction of the vial and the sun wheel was reversed every six minutes after a rest period of two minutes to ensure homogeneous grinding without overheating. The milled powders were mixed with Polyvinyl alcohol (PVA) as binder and then pressed into pellets of 10 mm diameter and 1 mm thickness under 2-MPa uniaxial hydraulic pressure. The pellets were sintered at 1000 °C for 2h. The corresponding ceramics so obtained for the two compositions will be abbreviated as KM0 and KM3. The Archimedes principle was used to measure the bulk density of these ceramics. X-ray Diffractometer (Philips Diffractometer PW 3020) with monochromatic CuK_α radiation (λ = 1.54178 Å) was used to characterize the crystalline phase of the ceramics. For electrical characterization, electroding was performed by painting silver paste on flat faces of the ceramic pellets and firing at 150 °C for 1h. The dielectric properties of the ceramics were measured by using an impedance analyzer (Wayne Kerr 4294A). The polarization versus electric field (P-E) hysteresis loops of the ceramics were recorded using an automated P-E loop tracer (AR Imagetronics, India) operating at 50 Hz. For piezoelectric measurements, the ceramic pellets were poled for 30 min at 120 °C in a silicone oil bath by applying dc electric field of 3 kV/mm. The piezoelectric constant d_{33} was measured by using a Piezo d_{33} meter (YE2730A d33 METER).

III. Results and Discussion

The values of bulk density obtained for KM0 and KM3 were 4.352 and 4.388 g/cm^2, respectively. Both the ceramic samples reached a density of over 95% of the theoretical density (TD, 4.51 g/cm^2) of $(K_{0.5}Na_{0.5})NbO_3$ [16], indicating that they are dense and well sintered. It can also be noted that the density of the ceramics improves with Mn^{4+} doping. MnO_2 acts as a sintering aid and introduces the liquid phase during the sintering process, which results in the higher density of the Mn-substituted KNN sample [30], [31]

Fig. 1 shows the room temperature XRD patterns of $(K_{0.485}Na_{0.5}Li_{0.015})(Nb_{0.98}V_{0.02})O_3 + x\ MnO_2$ (x = 0 and 0.03 wt. %) ceramics. The crystalline phase of the ceramics was of pure perovskite structure and no evidence of the formation of any secondary phase was observed. All the diffraction peaks can be indexed based on the standard X-ray pattern of polycrystalline orthorhombic $KNbO_3$ structure with *Amm2* space group JCPDS No. 71-0946 in the ICDD database, $KNbO_3$ being taken as a reference because it is iso-structural with KNN. The splitting of the (022) and (200) peaks at 2θ of ~45.5° with higher intensity counts for the (022) peak indicates that the crystal structure of the ceramics is orthorhombic [32]-[35]. Fig. 1 also depicts a slight shifting of the diffraction peaks towards higher angles indicating a small shrinkage of lattice cell volume as Mn^{4+} content increases in the ceramics. Partial substitution of Mn^{4+} with ionic radius (IR) = 0.54Å for Nb^{5+} (IR = 0.64Å) is expected to be primarily responsible for the altered unit cell dimensions. The observed shifting of diffraction peaks further supports the idea of Mn^{4+} substitution into the $(K_{0.5}Na_{0.5})NbO_3$ lattice to form a solid solution.

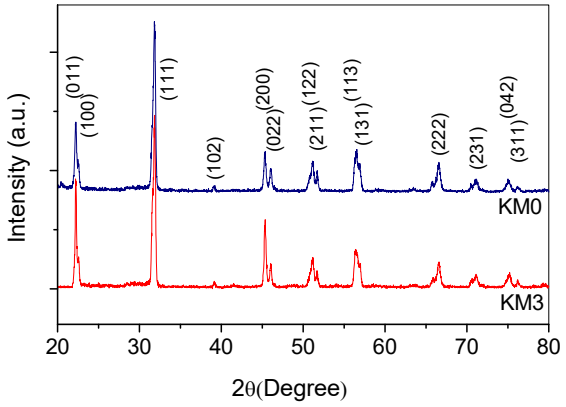

Fig. 1 XRD patterns of $(K_{0.485}Na_{0.5}Li_{0.015})(Nb_{0.98}V_{0.02})O_3 + x\ MnO_2$ (x = 0, and 0.03 wt. %) ceramics

Fig. 2 shows the temperature dependence of dielectric constant (ε) measured at 100 kHz for the two ceramic samples. It is seen that all the ceramics depict two dielectric peaks at about 150 °C and 410 °C. These peaks correspond to the phase transitions of orthorhombic-tetragonal (at T_{ot}) and tetragonal-cubic (at T_c), respectively. This observation confirms that the phase structure of both the ceramic samples prepared at room temperature has an orthorhombic symmetry, as discussed in XRD analysis. It can be remarked that the T_{ot} and T_c values for the ceramics are shifted slightly to higher temperatures due to Mn^{4+} doping. The change in these transition temperatures can be the evidence of Mn^{4+} dopants entering the lattice of $(K_{0.485}Na_{0.5}Li_{0.015})(Nb_{0.98}V_{0.02})O_3$ ceramics.

The values of room temperature dielectric constant (ε_{RT}) and dielectric constant maximum at the Curie temperature T_c (ε_{max}) are respectively 1318 and 2956 for KM0, and 1349 and 3802 for KM3. Thus, both the parameters ε_{RT} and ε_{max} increase as a result of Mn^{4+} doping in the ceramics. The observed increase in dielectric constant for KM3 is in agreement with its higher density. Such dependence of dielectric constant on density has been reported in other systems [23], [36].

Fig. 3 shows the typical hysteresis loops of polarization (P) versus applied electric field (E) plotted for some of the temperatures recorded for KM0 and KM3, measured at 50 Hz. It is seen in this figure that the shape of *P-E* hysteresis loops exhibits a strong dependence on the temperature for both the undoped and doped samples.

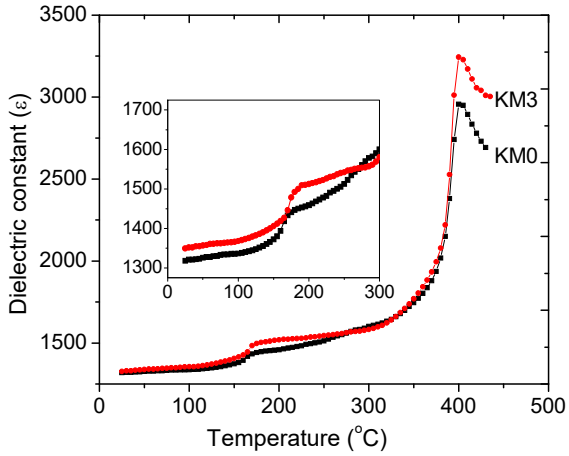

Fig. 2 Temperature dependence of dielectric constant (ε), measured at 100 kHz, for KM0 and KM3

For both samples, as the temperature increases, the hysteresis loops become more and more square-shaped and well-saturated indicating the improved ferroelectric behavior of the ceramics in the range of temperature studied. However, the shapes and sizes of the corresponding *P-E* loops at each temperature for the undoped and Mn^{4+} doped ceramic samples are quite different.

Fig. 4 depicts the plots of remnant polarization (P_r) versus temperature for the undoped and Mn^{4+} doped ceramic samples. As seen in Fig. 4, for KM3, the value of P_r increases gradually from 18.9 μC/cm^2 to 23.8μC/cm^2 as the temperature increases from 38 °C to 155 °C (i.e., around its T_{ot}). Similarly, for KM0, P_r increases gradually from 13.0 μC/cm^2 to 18.2 μC/cm^2 as the temperature increases from 38 °C to 155 °C. It is seen from Fig. 4 that the values of P_r are appreciably higher for KM3 than those for KM0 at each temperature of the temperature range mentioned above. This indicates that there is an improvement of ferroelectricity in the KM ceramics as a result of Mn^{4+} doping, in this range of temperature. It can be also noted that the variation in P_r over this temperature range is confined within a much narrower range for KM3 than that for KM0. This observation suggests that there is a great improvement in temperature stability of ferroelectricity for the Mn^{4+} doped ceramic, a desirable result from the point of view of its industrial applications in devices.

Fig. 5 shows the plots of coercive field (E_c) versus temperature for KM0 and KM3. As the temperature increases from 38 °C towards T_{ot}, E_c is found to decrease gradually from 7.0 kV/cm to 3.7 kV/cm for KM0, whereas for KM3, the corresponding decrease is observed to be from 5.9 kV/cm to 5.4 kV/cm. The lower values of E_c for KM3 indicate that the ferroelectric behavior of the ceramic becomes softer with Mn^{4+} doping. The significantly smaller range of variation in E_c over this wide range of temperature for KM3 suggests that the temperature stability of ferroelectricity is greatly improved in the Mn^{4+} doped ceramic as compared with the undoped ceramic. The appreciably low values of E_c with the values remaining almost unchanged over such a wide range of temperature can be of great use for the Mn^{4+} doped ceramic in various applications in electronic industry.

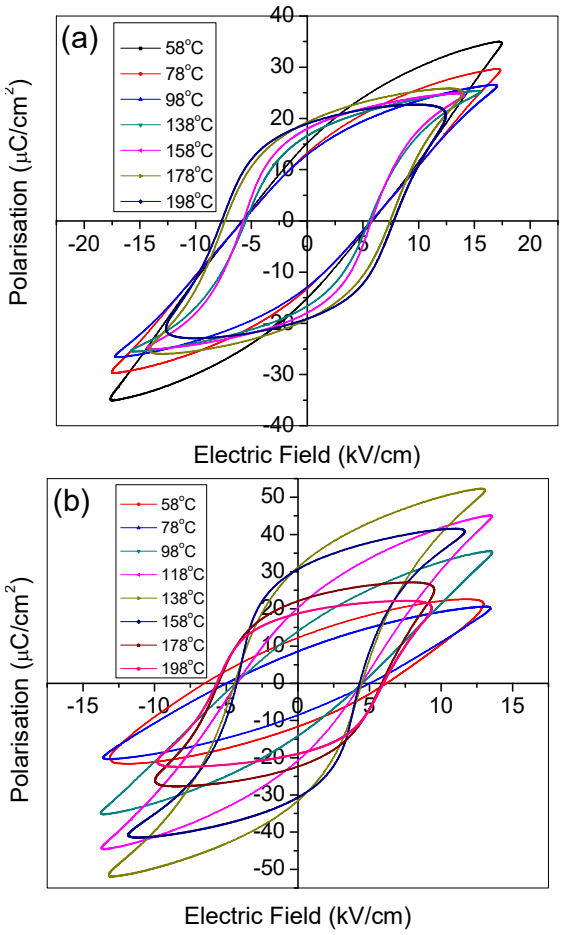

Fig. 3 P-E hysteresis curves at different temperatures, for (a) KM0, and (b) KM3, measured at 50 Hz

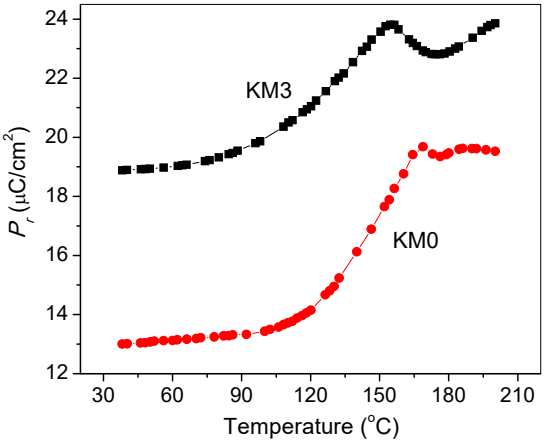

Fig. 4 Plots of P_r versus temperature versus temperature, for KM0 and KM3, measured at 50 Hz

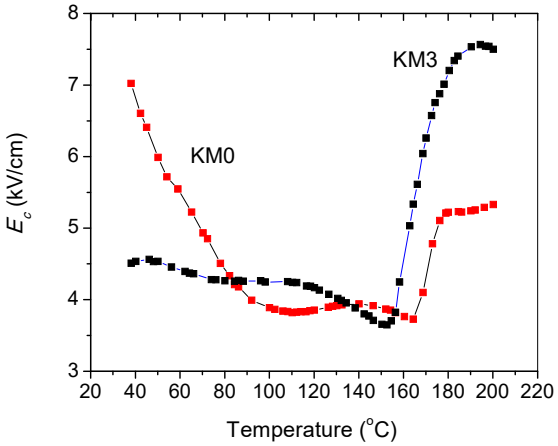

Fig. 5 Plots of E_c versus temperature, for KM0 and KM3, measured at 50 Hz

IV. Conclusions

Lead-free $(K_{0.485}Na_{0.5}Li_{0.015})(Nb_{0.98}V_{0.02})O_3 + x\ MnO_2$ (x = 0, and 0.03 wt.%) ceramics were synthesized by conventional air-sintering method. Both the ceramics exhibit pure perovskite structure with orthorhombic symmetry. Mn^{4+} doped ceramic exhibits higher density, room-temperature dielectric constant ε_{RT} and remnant polarization P_r. The remnant polarization P_r of the Mn^{4+} doped sample remains high in a narrow range of values from 18.9 μC/cm^2 to 23.8 μC/cm^2 over a wide range of temperature from about room temperature to the orthorhombic-tetragonal phase transition. On the other hand, the coercive field E_c remains significantly low for the Mn^{4+} doped sample, confined within a narrow range of values from 5.9 kV/cm to 5.4 kV/cm over the same range of temperature. The study reveals that an optimum amount of Mn^{4+} doping in $(K_{0.485}Na_{0.5}Li_{0.015})(Nb_{0.98}V_{0.02})O_3$ ceramic system can introduce desirable changes in its crystalline structure and morphology so as to enhance its ferroelectric behaviour and good thermal stability over a wide range of temperature.

Acknowledgment

The authors thank the Department of Science and Technology, Government of India (Research Project No. SR/S2/CMP-0017/2011) for financial support.

References

[1] B. Jaffe, "Piezoelectric Ceramics," New York: Academic Press, pp. 214-217, 1971.
[2] Y. Guo, K. Kakimoto, H. Ohsato, "Phase transitional behavior and piezoelectric properties of $(Na_{0.5}K_{0.5})NbO_3$–$LiNbO_3$ ceramics," *Appl. Phys. Lett.*, 85, pp. 4121–4123, 2004.
[3] B. Malic, J. Bernard, J. Hole, D. Jenko, M. Kosec, "Alkaline-earth doping in (K,Na)NbO_3 based piezoceramics," *J. Eur. Ceram. Soc*., 25, pp.2707–2711, 2005.
[4] J.F. Li,; K. Wang, B.P. Zhang, L.M. Zhang, "Ferroelectric and piezoelectric properties of fine-grained $Na_{0.5}K_{0.5}NbO_3$ lead-free piezoelectric ceramics prepared by spark plasma sintering," *J. Am. Ceram. Soc*., 89, pp.706–709, 2006.
[5] G.A. Smolensky, V.A. Isupov, A.I. Agranovskaya, N.N. Krainik, "New ferroelectrics of complex composition," *Sov. Phys. Solid State*, 2, pp. 2651–2654, 1961.
[6] T. Takenaka, K. Sakata, "New piezo- and pyroelectric sensor materials of $(BiNa)_{1/2}TiO_3$-based ceramics," *Sens. Mater.*, 1, pp. 123–131., 1988.
[7] H. Nagata, M. Yoshida, Y. Makiuchi, T. Takenaka, "Large piezoelectric Constant and High Curie Temperature of Lead-Free Piezoelectric Ceramic Ternary System Based on bismuth Sodium Titanate-Bismuth Potassium Titanate-Barium Titanate near the Morphotropic Phase Boundary," *Jpn. J. Appl. Phys*., 42, pp. 7401–7403, 2003.
[8] C.F. Buhrer, "Some properties of bismuth perovskites," *J. Chem. Phys*., 36, pp. 798–803, 1962.
[9] Y. Hiruma, H. Nagata, T. Takenaka, "Dielectric and Piezoelectric Properties of Barium Titanate and Bismuth Potassium Titanate Solid-Solution Ceramics," *J. Ceram. Soc. Jpn*., 112, pp. S1125–S1128., 2004.
[10] R.R. Neurgaonkar, W.F. Hall, J.R. Oliver, W.W. Ho, W.K. Copy, "Tungsten bronze $Sr_{1-x}Ba_xNb_2O_6$: A case history of versatility," *Ferroelectrics*, 87, pp. 167–179., 1988.
[11] M.J. Forbess, S. Seraji, Y. Wu, C.P. Nguyen, G.Z. Cao, "Dielectric properties of layered perovskite $Sr_{1-x}A_xBi_2Nb_2O_9$ ferroelectrics (A = La, Ca and x = 0, 0.1)," *Appl. Phys. Lett.*, 76, pp. 2934–2936, 2000.
[12] A. Ando, M. Kimura, T. Sawada, K. Hayashi, Y. Sakabe, "Piezoelectric and ferroelectric properties of the modified $SrBi_2Nb_2O_9$ ceramics," *Ferroelectrics*, 268, pp. 65–70, 2002.
[13] T. Sawada, A. Ando, Y. Sakabe, D. Damjanovic, N. Setter, "Properties of the Elastic Anomaly in $SrBi_2Nb_2O_9$-based Ceramics," *Jpn. J. Appl. Phys.*, 42, pp. 6094–6098, 2003.
[14] M. D. Maeder, D. Damjanovic, N. Setter, "Lead free piezoelectric materials," *J. Electroceram.* 13 pp. 385-392, 2004.
[15] Y. Saito, H. Takao, T. Tani, T. Nonoyaima, K. Takatori, T. Homma, T. Nagaya, M. Nakamura, "Lead-free piezoceramics," *Nature* 432 pp. 84-87, 2004.
[16] M. Kosec, D. Kolar, "On activated sintering and electrical properties of $NaKNbO_3$," *Mater. Res. Bull.* 10 pp. 335-340, 1975.
[17] R. Wang, R.J. Xie, K. Hanada, K. Matsusaki, H. Bando, M. Itoh, "Phase diagram and enhanced piezoelectricity in the strontium titanate doped potassium–sodium niobate solid solution," *Phys. Stat. Sol. A* 202 pp. R57-R59., 2005.
[18] R.E. Jaeger, L. Egerton, "Hot pressing of potassium-sodium niobates," *J. Am. Ceram. Soc.* 45, pp.209-213, 1962.
[19] G.H. Haertling, "Properties of hot-pressed ferroelectric alkali niobate ceramics," *J. Am. Ceram. Soc*. 50, pp. 329-330, 1967..
[20] L. Egerton, C.A. Bieling, "Isostatically hot-pressed sodium potassium niobate transducer material for ultrasonic devices," *Ceramic. Bull.* 47, pp. 1151-1156, 1968.
[21] E. Hollenstein, M. Davis, D. Damjanovic, N. Setter, "Piezoelectric properties of Li and Ta modified $(Na_{0.5}K_{0.5})NbO_3$ ceramics," *Appl. Phys. Lett*. 87, pp. 182905/1-182905/3, 2005.
[22] S. Zhang, J.B. Lim, T.R. Shrout, "Characterization of hard piezoelectric lead-free ceramics," *IEEE Trans Ultrason. Ferroelectr. Freq. Control.* 58, pp.1523-1527, 2009.
[23] K. Chandramani Singh, C. Jiten, R. Laishram, O.P. Thakur, D.K. Bhattacharya, "Structure and electrical properties of Li- and Ta-substituted $K_{0.5}Na_{0.5}NbO_3$ lead-free piezoelectric ceramics prepared from nanopowders," *J. Alloys. Compd.* 496, pp.717–722, 2010.
[24] D. Lin, K.W. Kwok, K.H. Lam, H.L.W. Chan, "Structure and electrical properties of $K_{0.5}Na_{0.5}NbO_3$-$LiSbO_3$ lead-free piezoelectric ceramics," *J. Appl. Phys.* 101, pp. 074111-074116, 2007.
[25] M. Matsubara, K. Kikuta, S. Hirano, "Piezoelectric properties of $(K_{0.5}Na_{0.5})(Nb_{1-x}Ta_x)O_3$–$K_{5.4}CuTa_{10}O_{29}$ ceramics," *J. Appl. Phys.* 97, pp. 114105 1-5, 2005.
[26] P. Guo, K. Kakimoto, H. Ohsato, "$Na_{0.5}K_{0.5}NbO_3$-$LiTaO_3$lead-free piezoelectric ceramics," *Mater. Lett.* 59, pp. 241-244, 2005.
[27] R. Gaur, A. Dhingra, S. Pal and K. Chandramani Singh, "Enhanced piezoelectric properties in vanadium-modified lead-free $(K_{0.485}Na_{0.5}Li_{0.015})(Nb_{0.88}Ta_{0.1}V_{0.02})O_3$ ceramics prepared from nanopowders," *Journal of Alloys and Compounds,* 625, pp. 284-290, 2015.
[28] H. Kishi, N. I. Kohzu, Y. Iguchi, J. Sugino, M. Kato, H. Ohsato, and T. Okuda, ''Occupational Sites and Dielectric Properties of Rare-Earth and Mn Substituted $BaTiO_3$,'' *J. Eur. Ceram. Soc.,* 21, pp. 1643–7, 2001.
[29] Y. Hou, M. Zhu, F. Gao, H.Wang, B. Wang, H. Yan, and C. Tain, ''Effect of MnO_2 Addition on the Structure and Electrical Properties of $Pb(Zn_{1/3}Nb_{2/3})_{0.20}$ $(Zr_{0.50}Ti_{0.50})_{0.80}O_3$ Ceramics,'' *J. Am. Ceram. Soc*., 87 (1), pp.847–50,2004.

[30] R. Rani, S. Sharma, R. Rai, and A.L. Kholkin, "Investigation of dielectric and electrical properties of Mn doped sodium potassium niobate ceramic system using impedance spectroscopy," *J. Appl. Phys.*, 110, No. 10, pp. 104102, 2011.
[31] L.G. Gusakova, V.M. Ishchuk, N.G. Kisel, D.V. Kuzenko, and N.A. Spiridonov, "Modified potassium–sodium niobate based lead-free piezoceramics," *Funct. Mater.*, 17, No. 4, pp. 528, 2010.
[32] M. Matsubara, T. Yamaguchi, W. Sakamoto, K. Kikuta, T. Yogo, S. Hirano, "Processing and piezoelectric properties of lead free $(KNa)(NbTa)O_3$," *J. Am. Ceram. Soc*. 88, pp.1190-1196, 2005.
[33] M. Matsubara, T. Yamaguchi, K. Kikuta, S. Hirano, "Effect of Li substitution of piezoelectric properties of potassium sodium niobate ceramics," *Jpn. J. Appl. Phys.* 44, pp. 6136-6142, 2005.
[34] N.M. Hagh, B. Jadidian, A. Safari, "Property-processing relationship in lead-free $(K,Na,Li)NbO_3$ solid solution systems," *J. Electroceram.* 18, pp. 339-346, 2007.
[35] G.C. Jiao, H.Q. Fan, L.J. Liu, W. Wang, "Structure and piezoelectric properties of Cu-doped potassium sodium tantalate niobate ceramics," *Mater. Lett.* 61, pp. 4185-4187, 2007.
[36] R. Gaur. K. Chandramani Singh, R. Laishram, "Structural and piezoelectric properties of barium modified lead-free $(K_{0.455}Li_{0.045}Na_{0.5})(Nb_{0.9}Ta_{0.1})O_3$ ceramics," *J. Mater. Sci.* 48, pp. 5607–5613, 2013.